

# Pico Gauges for Minimally Invasive Intracellular Hydrostatic Pressure Measurements<sup>1</sup>[C][W][OPEN]

Jan Knoblauch, Daniel L. Mullendore, Kaare H. Jensen, and Michael Knoblauch\*

Department of Organismic and Evolutionary Biology, Harvard University, Cambridge, Massachusetts 02138 (J.K., K.H.J.); School of Biological Sciences, Washington State University, Pullman, Washington 99164 (J.K., D.L.M., M.K.); and Department of Physics, Technical University of Denmark, Kongens Lyngby DK-2800, Denmark (K.H.J.)

Intracellular pressure has a multitude of functions in cells surrounded by a cell wall or similar matrix in all kingdoms of life. The functions include cell growth, nastic movements, and penetration of tissue by parasites. The precise measurement of intracellular pressure in the majority of cells, however, remains difficult or impossible due to their small size and/or sensitivity to manipulation. Here, we report on a method that allows precise measurements in basically any cell type over all ranges of pressure. It is based on the compression of nanoliter and picoliter volumes of oil entrapped in the tip of microcapillaries, which we call pico gauges. The production of pico gauges can be accomplished with standard laboratory equipment, and measurements are comparably easy to conduct. Example pressure measurements are performed on cells that are difficult or impossible to measure with other methods.

One of the most striking architectural variances of cells of different kingdoms is the presence of a cell wall. In plants, fungi, bacteria, protists, and some animal cells, the generation of an intracellular hydrostatic pressure via the interplay of osmotic potentials between extracellular and intracellular milieu, the selective permeability of the plasma membrane, and a supporting structure enclosing the cell allow for the development of a variety of effects critical for cell and tissue performance. For instance, the stiffness of plant or thallus parts, stomatal and nastic movements, long-distance assimilate transport, cell growth, seed distribution, penetration of tissues by parasites or predators, and others require cell pressures in the range 0.01 to 10 MPa and above (Howard et al., 1991; Tomos, 2000; Charras et al., 2005; Stewart et al., 2011). The determination of intracellular pressure, therefore, is of high interest for a variety of fields and has led to the development of several measurement techniques.

Recently, systems based on nanoindentation have been introduced (Forouzesh et al., 2013) and may be useful in the future, but parameters such as viscoelastic materials properties and the instantaneous elastic modulus need to be known, which are difficult to gather, and so far, several parameters need input from models rather than from

direct measurements. Another new development is based on implanted silicon chips (Gómez-Martínez et al., 2013). The size of the chip ( $4 \times 6 \mu\text{m}$ ) makes it suitable only for implantation into some animal cells but excludes it from use in cells surrounded by cell walls and cells sensitive to manipulation.

The most widely used approach is the cell pressure probe that consists of a microcapillary tube filled with silicone oil, which is connected to a pressure transducer and a piston (Hüsken et al., 1978; Tomos and Leigh, 1999). Insertion of the narrow capillary tip into a cell leads to an influx of cellular fluid into the tube, which is visible as a movement of the meniscus at the boundary of the silicone oil and the cytoplasm. The cytoplasmic fluid is then forced back into the cell by increasing the pressure via the piston until the meniscus reaches its equilibrium position. Finally, the pressure is recorded by means of the pressure transducer (Tomos and Leigh, 1999).

Despite the great success of the cell pressure probe system and numerous excellent investigations that are crucial for our current understanding of cell function, there are several cell types that are difficult or impossible to measure with this system. The shock induced by impalement of the needle, which may cause an initial pressure release by flow of the cytoplasm into the needle tip, may lead to turgor changes and false readings. For example, despite numerous efforts, we were not able to apply the cell pressure probe to measure sieve tube turgor due to rapid injury responses.

One of the reasons is the significant difference in volume between the cell and the cell pressure probe. Typical cell pressure probes comprise a glass capillary tube and an oil reservoir with a combined volume of at least 10 to 100  $\mu\text{L}$  (the glass capillary accounts for approximately 5  $\mu\text{L}$ ). A pressure of 1 MPa compresses the probe fluid by about 0.1%, corresponding to a volume change of 10 to 100 nL. By contrast, cell volumes are

<sup>1</sup> This work was supported by the National Science Foundation (grant nos. IOS 1146500, DMR 0820484), and the Carlsberg Foundation (grant no. 2013\_01\_0449).

\* Address correspondence to knoblauch@wsu.edu.

The author responsible for distribution of materials integral to the findings presented in this article in accordance with the policy described in the Instructions for Authors ([www.plantphysiol.org](http://www.plantphysiol.org)) is: Michael Knoblauch (knoblauch@wsu.edu).

[C] Some figures in this article are displayed in color online but in black and white in the print edition.

[W] The online version of this article contains Web-only data.

[OPEN] Articles can be viewed online without a subscription.

[www.plantphysiol.org/cgi/doi/10.1104/pp.114.245746](http://www.plantphysiol.org/cgi/doi/10.1104/pp.114.245746)

usually in the picoliter to lower nanoliter range. Thus, the probe can absorb many times the volume of cells under investigation. To minimize the effects, the cell pressure probe can be pressurized prior to impalement just below the expected turgor pressure, which in many cases prevents a major loss of turgor and cell sap. However, it should be noted that the compression of the oil reservoir still allows an influx of 100 pL to 1 nL of cell fluid if the prepressure applied to the cell pressure probe differs by only 10 kPa from the cell turgor pressure. This makes it difficult to measure cells if the turgor value is difficult to anticipate due to extremely variable and high turgor in cells such as sieve elements and guard cells.

The cause of the problems described above is the large liquid volume in the system, which exceeds the cell volume by several orders of magnitude. Our aim was to prevent these problems by minimizing the interacting volume. Here, we report on a method that is based on the compression of nanoliter-, picoliter-, or even femtoliter-sized oil volumes trapped in the tip of microcapillaries. Production of the capillaries is a fast and simple process. Pico gauges allow accurate measurements in basically all cell types, including those that are difficult or impossible to measure with standard cell pressure probes or other systems.

## RESULTS AND DISCUSSION

The pressure-dependent compression of fluids is a ubiquitously used indicator to calculate pressure changes. To record cell turgor, the compressed oil volume should be significantly lower than the cell volume, ideally below 1%, to prevent or minimize the induction of injury responses. The volume of cells differs by several orders of magnitude. The volume of small cells such as plant guard cells is in the lower picoliter range, while large parenchyma and epidermis cells can reach nanoliter volumes and above. Extremes are multinucleated single cells of macroalgae such as *Chara*, *Nitella*, and *Caulerpa* spp., with volumes of microliter to milliliter and above (Hüsken et al., 1978; Mine et al., 2008).

### Liquid Compression-Based Pressure Sensors

The compressibility of liquids is minor compared with that of gases. However, in capillaries that taper, minute changes can be visualized in the tip of the cone. The isothermal compression of the probe fluid can be described by the relation:

$$K = -V \frac{\Delta p}{\Delta V} \quad (1)$$

where  $K$  is the bulk modulus of the liquid,  $V$  is the initial volume of compressible liquid,  $\Delta p$  is the applied pressure difference, and  $\Delta V$  is the volumetric change (Timoshenko, 1951). The bulk modulus of degassed water is  $2.15 \times 10^9$  Pa, which results in a relative compression ( $\Delta V/V$ ) of 0.046% at 1 MPa and 293 K. Silicone

oil is softer; therefore, the bulk modulus is slightly lower. In order to visualize the compression with the microscope, an interface of cell sap and the filling material is required, thus excluding all water-soluble liquids. The interface between oils and cell fluids is well visible due to differences in optical density, and the effects of surface tension are minor, making them a good choice. If the view of the meniscus is blocked (e.g. by multiple cell layers), oils can be stained with fluorophores to provide contrast and the experiment can be conducted using a fluorescence microscope.

To construct a liquid-filled pressure sensor, the compressible volume of the liquid has to be adjusted according to the cell type to be measured. Since the compressibility of an oil-filled system is roughly 1/1,000 at 1 MPa, the compressible liquid volume should not exceed 10 cell volumes to limit the maximum influx to about 1% of the cell volume. Therefore, the production of needles with volumes in the nanoliter, picoliter, and femtoliter range is required.

### Production of Pico Gauges

Control over the production of pico gauges with such small volumes is conducted by the solidification of glue after generation of the desired oil volume in the tip. UV light-curable glues allow time-independent handling and the induction of glue solidification at any given time point. Production occurs with a standard fluorescence microscope, which provides the application of UV light at various intensities and the simultaneous observation of the oil volume. We have developed two basic methods for the production of pico gauges with different volume ranges (Fig. 1; Supplemental Movies S1 and S2).

#### Method A

The first method employs oil and glue that are consecutively filled into the tip by means of microloaders (Supplemental Appendix S1). Application of pressure to the back end of the capillary pushes the oil through the tip until the desired volume of oil is generated (Fig. 1, A and B), and the glue is cured by the application of UV light, which fixes the oil volume in place (Fig. 1, C and D; Supplemental Movie S1). Pressure to the back end of the capillary can be applied with standard microinjection or cell pressure probe devices in order to drive oil through the needle tip. If those are not available, custom-built devices as simple as a syringe piston controlled by a micrometer screw and connected to the capillary can be used to apply pressure and to control flow in the capillary. All necessary information on devices to produce and handle pico gauges is given below and in Supplemental Appendix S1. The method is suitable to produce medium (picoliter) to large (nanoliter and above) volumes.

#### Method B

The second method employs the shrinkage induced by the resin's transformation from a liquid into a solid

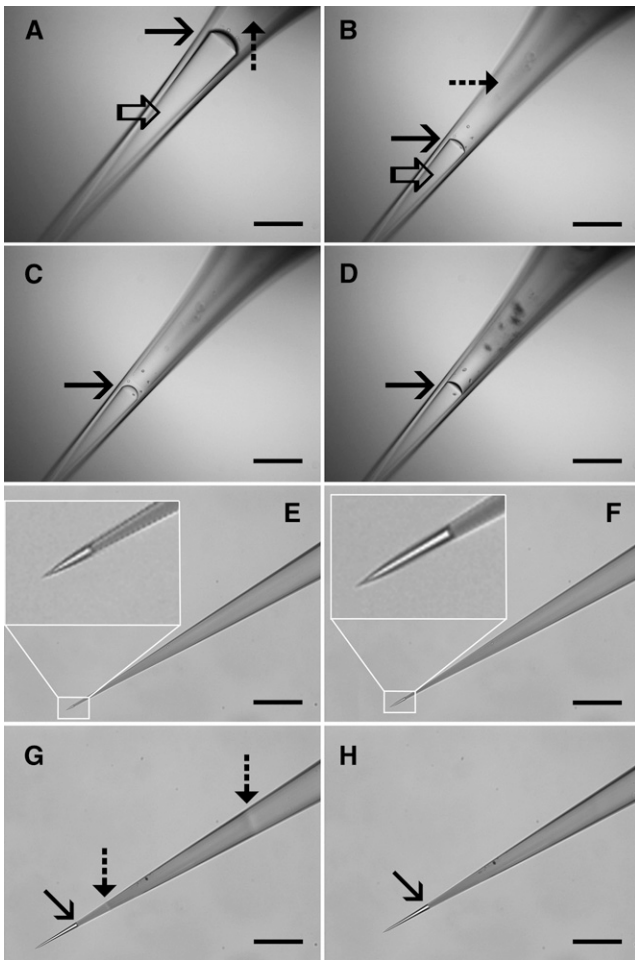


**Figure 1.** Production of pico gauges. A to D, Pico gauge production by pressure (method A). A capillary tip is consecutively filled with 10 centistokes (cSt) silicone oil (open arrow) and Loctite 3492 resin (dashed arrow) and submerged into oil (A). The oil/resin boundary is well visible (solid arrow). Application of pressure pushes the oil through the tip and the oil/resin boundary moves forward (B–D). Once the desired oil volume is reached, pressure is reduced, UV light is turned on, and the resin is cured. E to H, Pico gauge production by resin shrinkage (method B). A microcapillary tip is filled completely with resin (in this case, Loctite 352). Submerging the tip into water causes capillary forces to pull in water slowly (E and F, insets). Application of UV light (G) restricted to a small area by the field diaphragm initiates glue curing, indicated by a change in the refractive index (dashed arrow). Shrinkage of the resin pulls water into the tip (solid arrow). Opening the diaphragm cures the remainder of the resin (H). After production of a small volume, the water is exchanged for oil. Bars = 200  $\mu\text{m}$ .

phase during polymerization. In this case, the capillary tip is completely filled with the resin and then submerged into the filling fluid (Fig. 1, E and F). To control the oil volume to be generated, the field diaphragm of the microscope is closed to the smallest size and UV light is applied to form a clot (Fig. 1G). Then, the remainder of the glue toward the tip is cured, causing the generation of tension in the tip, which results in fluid being pulled in (Fig. 1H; Supplemental Movie S2). Forming the clot

closer or farther away from the tip opening allows control of the final volume. This method allows the production of medium to extremely small volumes (low femtoliter volumes can be generated; Fig. 1).

A large variety of resins are available, and several appropriate products can certainly be found. However, we would recommend low-viscosity (method A) to medium-viscosity (method B) methacrylate or methacrylate/urethane/acrylate glues with relatively high amounts of photoinitiator to provide quick curing. The glues that worked best for us so far are Loctite 3492 for method A and Loctite 352 for method B. The glues are widely available at moderate costs. In all cases, it is recommended to use low-viscosity silicone oil (e.g. 10 cSt). Higher viscosity oil will increase production times significantly due to slow flow through the tip. This is especially the case when pico gauges with small tip sizes are produced.

Both procedures are rather simple, and the production of multiple capillaries per hour is standard.

### Storage

Pico gauges can be stored indefinitely, but storage should always occur with tips submerged in oil (Supplemental Appendix S1). For certain experiments, it is desirable to have the tip filled with fluorescent oil. A cheap and readily available option is fluorescent tracer to detect oil leaks in cars, such as Traceline dye lite or NAPA UV dye. It can be added to the oil in low quantities without changing the elastic modulus noticeably. Other hydrophobic fluorescent dyes, like 1,6-diphenyl-1,3,5-hexatriene, work as well, but they are more expensive. In any case, it is crucial that unstained oil is used during the production procedure. The photoinitiator of the glue destroys any fluorescent dye (that we tested) when UV light is applied. Instead, after production with unstained oil, the pico gauges are stored in fluorescent oil (Supplemental Appendix S1), which permits the diffusion of sufficient amounts of dye into the needle tip and the removal of remaining photoinitiator within about 1 d (depending on tip size).

### Transfer and Handling

Transfer through air and mounting in the micromanipulator may induce quick volume fluctuations in the needle tip due to minor temperature alterations by air convection or the body heat of the investigator. This can result in the loss of oil when it is pushed out of the tip at higher temperature and air bubble generation when it is pulled back in. Therefore, we recommend storage of the needles at 4°C or lower temperatures. The temperature-induced expansion of the oil during transfer from cold to warmer environments results in a minute outflow of oil from the tip until it is submerged in medium. Alternatively, a stream of cold air can be blown on the needle tip during transfer (Supplemental Appendix S1). Once submerged in the medium, the liquid serves as a very effective temperature buffer. Only minor volume changes over extended periods will occur that do not influence

the accuracy of measurements (see below). If, however, measurements in air or steady-state measurements are desired, a temperature-controlled environment is required.

### Pressure Measurement

To measure turgor pressure, the capillary is impaled into a cell and the compression of the oil volume within the tip is recorded. The minimum instrument outfit is a microscope equipped with a micromanipulator and a digital camera.

To calculate the intracellular pressure from Equation 1, three parameters need to be known: (1) the bulk elastic modulus of the compressed liquid; (2) the total oil volume in the capillary tip at ambient pressure; and (3) the volumetric change after pressure application.

### Elastic Bulk Modulus

The elastic bulk modulus of a specific silicone oil is a material property that usually can be acquired from the manufacturer. However, industrial measurement of elastic bulk modulus occurs at high pressures and under specific conditions like high vacuum, which differ from environments suitable for cell biological experiments. For example, gases dissolve in liquids depending on their chemical composition and the surrounding pressure. If the oil is degassed prior to the measurement, gas will diffuse into the needle tip during transfer and elastic bulk modulus will change as a function of time until the measurement is conducted. The effect is minor when measurements are taken within a few minutes but can be significant over extended periods. In addition, minor amounts of glue diffuse into the oil, forming a visible meshwork when cured, and the glass of the micropipette wall will expand when pressurized. To provide a setup for general application, we measured the bulk modulus for the system silicone oil 10 cSt, Loctite 3492 or Loctite 352 at atmospheric pressure, in a custom-built microscope pressure device that allows controlled pressure application of up to 2.5 MPa (Supplemental Appendix S1). For the system 10 cSt oil (stored at atmospheric pressure), Loctite glue, and standard borosilicate glass capillaries, elastic bulk modulus is  $0.782 \pm 0.003$  GPa ( $n = 69$ ). In comparison, elastic bulk modulus of pico gauges filled with 50 cSt and stored at 70 kPa is  $0.852 \pm 0.003$  GPa ( $n = 205$ ). Changing the glass type and diameter or changing the glue did not induce noticeable effects. For example, the radius of the glass capillary (elastic modulus of approximately 10 GPa) will increase by less than 0.05% at a pressure of 1 MPa. However, changing the oil type may induce significant errors. Therefore, we recommend to either use the system reported here or to measure elastic bulk modulus for alternative combinations.

### Oil Volume and Pressure-Induced Volumetric Change

The experiment itself is rather simple. The needle tip is directed in front of a cell wall and a movie is captured

during impalement (Fig. 2; Supplemental Movies S3–S5). Because of the small volume entering the tip, the measurement is usually completed within milliseconds. The needle can be reused as long as it is not clogged. Oil expansion to its original volume after retraction of the pico gauge at the end of an experiment indicates that the needle tip is open (Supplemental Movie S5). In a standard tissue, it is no problem to conduct multiple individual measurements within minutes.

To measure volumetric change, two images, one before and one after cell impalement, are extracted from the movie and overlaid using computer software such as ImageJ or Photoshop (Fig. 2C). The volume difference is then extracted using a lasso tool to demarcate the boundaries of the alteration in oil volume (Fig. 2D). Extraction of the demarcated area provides a two-dimensional surface of pressure-induced volume change. In order to translate the extracted area into a volume, a solid of revolution is generated by rotating the area around its axis of symmetry (Fig. 2E) using a custom software package (bubvol; Supplemental Software S1; test images are provided in Supplemental Images S1 and S2).

To calculate total oil volume, a snapshot of the needle tip containing the compressible oil volume is taken (Fig. 1, D and H), the oil volume is extracted (Fig. 2F), and the volume is calculated using bubvol as described above.

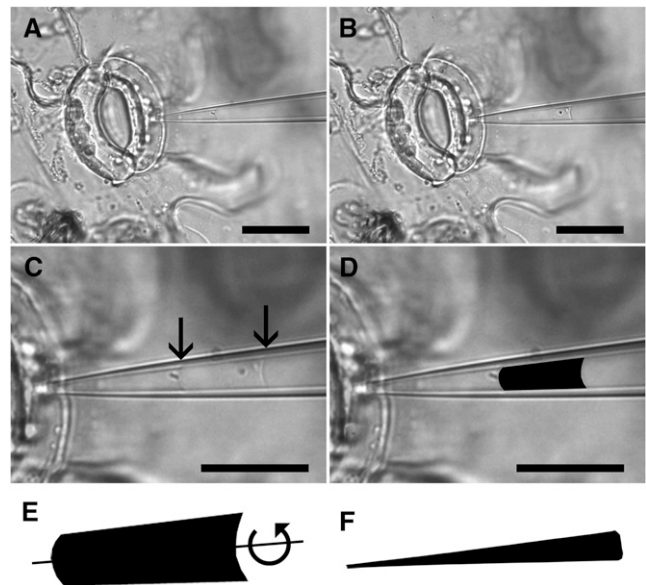


**Figure 2.** Pico gauge pressure measurement procedure. A pico gauge measurement is conducted in a guard cell. Two images, one before (A) and one after (B) pico gauge impalement, are extracted from a movie taken from the experiment. The two images are overlaid (C) with 50% opacity to make both images and oil menisci (arrows) visible. Afterward, the area of compression is extracted (D), and volumetric change is extracted by forming a solid of revolution by rotating the extracted area around its axis of symmetry (scheme in E) using software provided as Supplemental Appendix S1. The same is done with the total pico gauge oil volume to receive the volume (V) in Equation 1 (F). Note that E and F are not to scale. Bars = 25  $\mu\text{m}$  (A and B) and 20  $\mu\text{m}$  (C and D).

The entire procedure is relatively simple, and numerous measurements and calculations can be conducted within 1 d. A detailed step-by-step instruction is provided in “Materials and Methods.”

### Pico Gauge Accuracy Test

To test our system versus an established method, we used large, easy-to-measure onion (*Allium cepa*) epidermis cells to simultaneously measure turgor pressure via a cell pressure probe and a pico gauge. The experiment in Figure 3 and Supplemental Movie S3 was conducted at 630 $\times$ , showing the significant influx of cytoplasm when the needle of the cell pressure probe is impaled (Fig. 3, A and B). Pico gauge impalement, on the other hand, induces a minor influx well below 1% (volumetric change was 811 fL versus approximately 1.5 nL cell volume) of the cell volume (Fig. 3, C and D). In each of the three experiments, the measured pressure difference between the cell pressure probe and the pico gauge was in the range of 0.01 MPa (0.52 MPa [pressure probe] versus 0.518 MPa [pico gauge], 0.59 MPa [pressure probe] versus 0.597 MPa [pico gauge], and 0.78 MPa [pressure probe] versus 0.791 MPa [pico gauge]).

### Pico Gauge Measurements

#### Example 1: Pico Gauge Measurement of Turgor in Highly Sensitive, High-Pressure Cells

As described above, most plant, fungi, and protist cells are below the size that is regarded as suitable for cell pressure probe measurements. Although a number of theories on cell and organismal function contain a pressure component, accurate measurements are actually lacking. A classical example is the pressure-flow hypothesis proposed by Münch (1930), in which a pressure differential is thought to drive the long-distance transport of photoassimilates. Despite 85 years of research, the pressure-flow hypothesis still rests on its plausibility rather than on experimental proof (Knoblauch and Peters, 2010), which is a surprising fact, given that the phloem is a critical element and that the majority of food consumed by humans has passed through the phloem at one point. The problem is based on the small cell size and fast injury response of sieve tubes when cell pressure probes are impaled, leading to false readings.

To demonstrate the capabilities and convenience of pico gauge measurements, we decided to provide proof of principle by measuring hydrostatic pressure in translocating sieve elements. We prepared sieve elements for in vivo observation on intact plants (Knoblauch and van Bel, 1998). We used *Vicia faba* plants that contain forisomes as an indicator for the functional state of sieve tubes (Knoblauch et al., 2001, 2003). Impalement of a pico gauge provided an instant pressure reading (Fig. 4; Supplemental Movie S4). The cell recognized the impalement, and the forisome switched into its high-volume state. However, the quick, subsecond pressure reading by

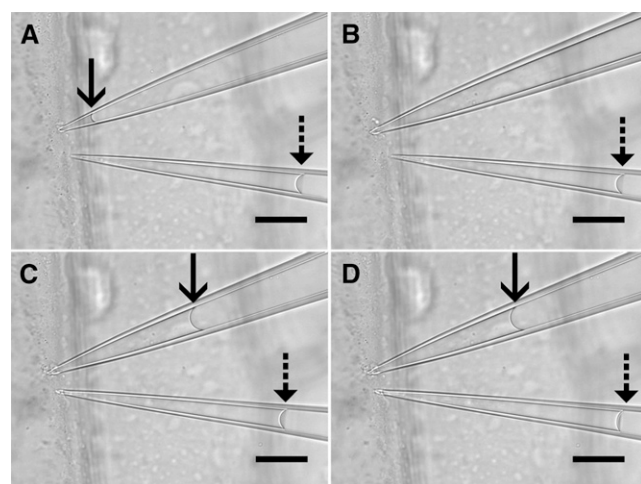


**Figure 3.** Simultaneous turgor pressure measurement with a cell pressure probe and a pico gauge. The four frames are taken from Supplemental Movie S3. A, The tips of a cell pressure probe (top pipette) and a pico gauge (bottom pipette) are located at the cell wall of an onion epidermis cell. The oil/water interfaces in the cell pressure probe (solid arrow) and the pico gauge (dashed arrow) are well visible. B, Impalement of the cell pressure probe leads to inflow of cell fluid into the tip and pushes the interface out of the visible area. C, Adjustment of the pressure via the piston increases the pressure in the probe, forcing cell sap back into the cell. The probe pressure is adjusted until the meniscus is stationary, and the pressure reading is taken. D, Impalement of the pico gauge leads to a slight compression of the oil, which is indicated by an instant movement of the oil/water interface. Bars = 25  $\mu$ m.

the pico gauge outruns the cellular reaction. We conducted eight sieve tube pressure readings within 90 min. The average pressure measured was 0.97 MPa.

#### Example 2: Pico Gauge Measurement of Turgor and Membrane Permeability in Small-Volume, High-Pressure Cells

Guard cells have a central function in controlling transpiration and gas exchange in plants. They are difficult to measure with cell pressure probes (Franks et al., 1998, 2001; Tomos, 2000; Franks, 2003) due to their small size, high turgor, and complex cell structure. We measured guard cell turgor with pico gauges (Fig. 2; Supplemental Movie S5; calculated pressure, 1.4 MPa) with relatively large volume compared with the cell volume to extract data on membrane permeability and pressure.

The compression of oil in the pico gauge after impalement increases the effective cell volume, which results in a drop of turgor and relaxation of the cell wall. Water will flow into the cell to equilibrate osmotic potentials and cell wall elasticity to resume hydrostatic pressure (Tomos and Leigh, 1999).

This process usually occurs in milliseconds when the volumetric change is below 1% of the cell volume but may take seconds when higher volumetric changes are induced. Figure 5 shows the time course of volumetric change from Supplemental Movie S5. Volumetric change is about 212 fL and therefore about 4% of the total guard

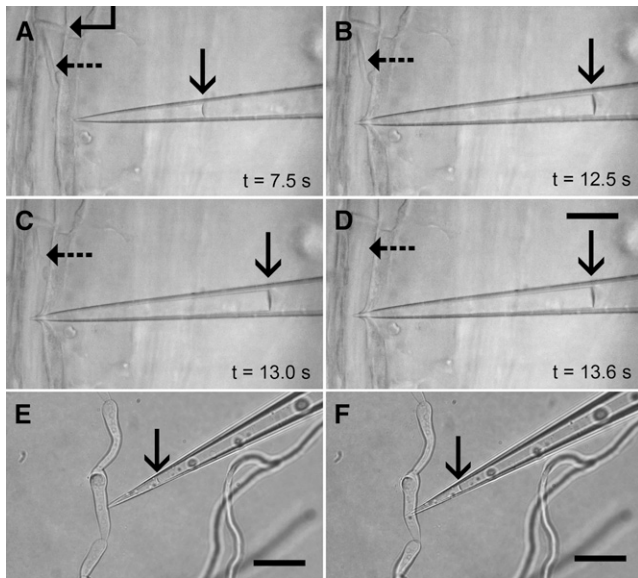


**Figure 4.** Pico gauge pressure measurement in sieve element and fungal cells. A to D, Four frames extracted from Supplemental Movie S5. A, A pico gauge tip is located in front of a sieve element with a sieve plate (angled arrow) and a forisome in the low-volume state (dashed arrow), indicating uninjured conditions. The oil/water interface in the pico gauge is marked by the solid arrow. B, Impalement of the pico gauge into the sieve element leads to an instant compression of the oil, which provides the pressure reading. C and D, The forisome switches into the high-volume state within 1 s, but the measurement is already completed before the forisome blocks the tube. E and F, Two frames extracted from Supplemental Movie S6 showing a pico gauge measurement in a fungal hyphae cell with a volume of only about 900 fL. The compression of the pico gauge fluid is minor (23 fL) but sufficient for a pressure calculation. The oil/water interface is shown by the arrows. Bars = 25  $\mu\text{m}$ .

cell volume of 5 pL. The equilibration takes about 3 s to complete. Analysis of the turgor recovery curve by measuring a series of movie frames after impalement allows the extraction of information on turgor and on membrane permeability.

### Example 3: Pico Gauge Measurement of Turgor in Small, Low-Pressure Cells

Fungal cells are well suited to manipulate turgor by extracellular osmotica because turgor control does not occur at least over short periods (Money and Harold, 1992; Harold et al., 1996). We used *Alternaria* spp. hyphae at an osmotic potential of the medium of 0.24 mosmol  $\text{kg}^{-1}$ . Figure 4, E and F, and Supplemental Movie S6 show the impalement of a pico gauge with a volume of 126 pL into a hyphae cell with a volume of only 900 fL. The low pressure in the hyphae results in a volumetric compression of 23 fL, which indicates a pressure of 0.14 MPa.

### Error Correction and Error Prevention

Pico gauge measurements lead to a series of events inside the cell and inside the needle. Initially, pico gauges

are filled with oil. When the tip is submerged into medium, capillary forces pull in water and compress the oil slightly. In addition, minor temperature differences between medium and the pico gauge (including oil and the glass wall) will lead to a slight movement of the medium/oil interface until temperature equilibrium is reached, which occurs usually within fractions of a second. However, the precise location of the medium/oil interface is not controllable.

One error that may need correction under certain circumstances is given by capillary forces and surface tension. The pressure at work is indicated by the curvature of the meniscus at the medium/oil interface, which can be calculated by the Young-Laplace equation:

$$\Delta p_{\text{stl}} = \frac{2\gamma}{r} \quad (2)$$

where  $\gamma$  is the surface tension of the water/oil interface (approximately 25  $\text{mN m}^{-1}$ ) and  $r$  is the radius of the curvature. The radius of curvature is measured by drawing a circle into the image that fits the curvature of the oil surface (Fig. 6) and measuring the radius of this circle.

Impalement of the pico gauge into a cell leads to compression of the oil and movement of the meniscus.

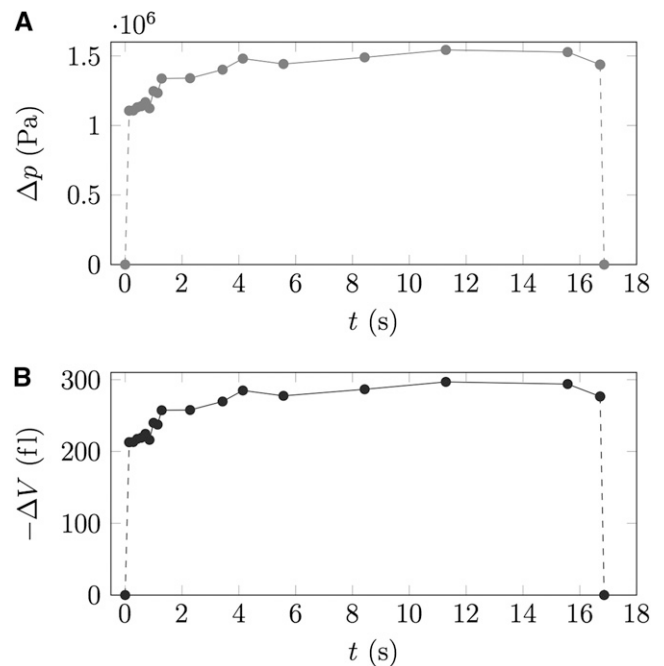


**Figure 5.** Extraction of membrane permeability from pico gauge measurements. Nineteen individual frames over the course of 17 s were extracted from Supplemental Movie S5, and the turgor recovery curve ( $\Delta p$ ; A) as well as the volumetric change ( $-\Delta V$ ; B) were plotted versus time. Since cell volume, cell surface area, and volumetric change over time can be measured, the membrane permeability can be extracted from the data.

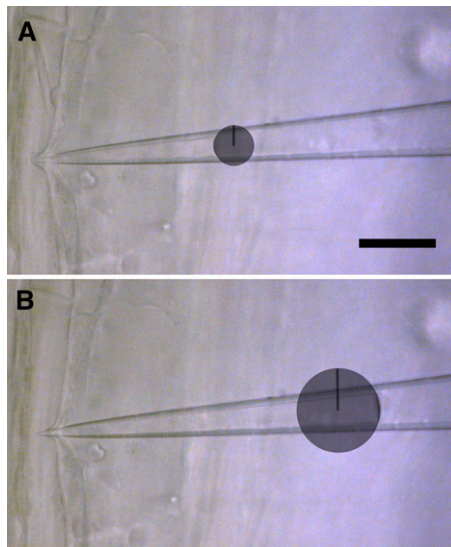


**Figure 6.** Correction for surface tension-induced errors. The effect of capillary forces and surface tension can be corrected by drawing a circle that fits the curvature of the oil/water interface and measuring its radius. The difference between the curvature before and after impalement provides a correction factor to be subtracted from the calculation. Bar = 25  $\mu\text{m}$ . [See online article for color version of this figure.]

Due to the cone shape of the needle, the form of the meniscus changes, which also changes the surface tension applied (Fig. 6B). Extracting  $r_2$  and calculating  $\Delta p_{\text{st}2}$  using Equation 2 allows correction by calculating the difference between the initial pressure applied by surface tension and the pressure applied by surface tension after impalement using Equation 3:

$$\Delta p_{\text{st}} = p_{\text{st}1} - p_{\text{st}2} \quad (3)$$

$\Delta p_{\text{st}}$  is the final correction factor that is subtracted from the calculated pressure because surface tension is an additional force. In almost all cases, this correction factor is negligible. An example is given in Figure 6 extracted from Supplemental Movie S4. With  $r_1 = 6.8 \mu\text{m}$ ,  $r_2 = 13.7 \mu\text{m}$ , and  $\gamma_{\text{water/oil}} = 25 \text{ mN m}^{-1}$ ,  $\Delta p_{\text{st}}$  is only 0.0018 MPa, compared with 0.97 MPa calculated cell turgor. However, it should be pointed out that the error increases with smaller tip diameter (the closer the meniscus is located toward the tip) and with increasing cone angle of the capillary. For example, a meniscus curvature with a radius of 1  $\mu\text{m}$  induces a pressure of 0.025 MPa.

Another, and in many cases more important, error is induced by the water volume in the pico gauge tip. During the process of impalement, the water body of the pico gauge becomes part of the effective cell volume. The increase in volume and the compression of the oil leads to an initial drop in turgor. The cell will take up water until turgor is regained, but because cell osmotica diffuse throughout the water body of the cell/pico gauge system, the dilution leads to a reduced

pressure reading. The error is minor as long as the pico gauge water volume is small compared with the cell volume. If necessary, the error can be corrected by extracting the volume of the pico gauge water content  $V_{\text{pg}}$  in relation to the cell volume  $V_c$  and using Equation 4:

$$P_{\text{turgor}} = P_{\text{calc}} \left( 1 + \frac{V_{\text{pg}}}{V_c} \right) \quad (4)$$

where  $P_{\text{calc}}$  is the calculated pressure from a pico gauge experiment and  $P_{\text{turgor}}$  is the turgor before impalement of the pico gauge (the cell turgor). In most cases,  $P_{\text{calc}}$  and  $P_{\text{turgor}}$  will be almost identical, especially if the cell volume-pico gauge water content ratio is below 1%. In experiments like the guard cell measurement in Supplemental Movie S5 as well as Figures 3 and 5, the error can be in the lower percentage range and correction may be appropriate.

Another error that may occur is concerned with the accuracy of the extraction of the area of volumetric change before and after impalement of the pico gauge. It is crucial to keep the pico gauge in focus. Volumes that approach pixel sizes with edge lengths close to the diffraction limit will have increasing errors. The smallest volumetric change we measured so far was 23 fL in Supplemental Movie S6. This volume contains about 1,500 cubic pixel, each with an edge length of 230 nm (diffraction limit). We compared calculations of the same measurements performed by three individuals. The error between the calculations was below 3%.

## CONCLUSION

The cell pressure probe is an excellent tool to acquire data on parameters such as cell turgor, cell wall elasticity, and membrane permeability and has been optimized for a number of cell types over the last decades (Steudle and Zimmermann, 1977; Hüsken et al., 1978; Cosgrove 1981, 1985, 1993; Shackel and Brinckmann, 1985; Cosgrove et al., 1987; Oparka et al., 1991; Ye and Steudle, 2006; Wada et al., 2014). Unfortunately, some cell types show rapid injury responses, which make it difficult or impossible to apply this method. We have developed a minimally invasive system for hydrostatic pressure and membrane permeability measurements in basically any cell type. Besides the small volumetric inflow of cell sap, the ability to measure in milliseconds outruns potential injury responses in most cell types even if they occur. The only cells that are not measureable are cells with exceptionally thick cell walls that cannot be penetrated by microcapillaries and cells that require the visualization of volumetric changes below the diffraction limit (e.g. bacteria cells). Otherwise, the method is suitable to measure any cell type at any given hydrostatic pressure. Detailed instructions on the general handling of pico gauges are provided in Supplemental Appendix S1.

## MATERIALS AND METHODS

### Pico Gauge Production Method A

Microcapillaries were pulled from borosilicate glass, 1-mm o.d. and 0.5-mm i.d. without filament (Harvard Apparatus), with a Sutter Instruments laser puller (model P-2000) to a final tip size of 0.2 to 0.5  $\mu\text{m}$ . The capillary tips were filled from the back end with silicone oil 10 cSt (378321; Sigma-Aldrich) by means of custom-built microloaders (Supplemental Appendix S1). After filling the tip with silicone oil, a drop of Loctite 3492 glue was added through a microloader just behind the oil. The capillary was mounted into a custom-built pressure injector, the tip was dipped into silicone oil 10 cSt, and about 1 MPa of pressure was applied to drive oil through the tip (Supplemental Movie S1). Flow was monitored with a fluorescence microscope (DM LFSa; Leica). Once the desired oil volume was reached in the tip, UV light was applied via filter block D of the fluorescence microscope to stop flow and cure the resin. It is important to note that the needle tip needs to be submerged into silicone oil during production, because curing of the resin causes shrinkage of the glue, which results in back flow of oil. If the needle is not submerged, air will be pulled in.

### Pico Gauge Production Method B

Capillaries were pulled as described above. The capillaries were back filled with Loctite 352 glue by means of microloaders (Supplemental Appendix S1), the resin was pushed into the tip, and the needle was submerged into double distilled water. Slow inflow of water due to capillary forces was monitored with a Leica DM LFSa fluorescence microscope (Supplemental Movie S2). Application of UV light induced curing and shrinkage of the glue, which results in tension in the capillary and uptake of water until the glue is fully cured. Control of the final volume is achieved by directing the UV light closer or farther away from the tip (Supplemental Movie S2). After glue curing, pico gauges were stored in air for about 30 min to allow water in the tip to evaporate. Air-filled pico gauges were submerged in oil, and the pressure applied by surface tension between oil and air leads to a slow dissolution of air until the entire tip is filled with oil. This takes about 1 d for tips with volumes in the low picoliter range. To speed up the process, or to fill tips with larger volumes, pressure can be applied in a pressure bomb or similar device. Alternatively, repeated application of vacuum and atmospheric pressure accelerates oil filling. In principle, pico gauge production by method B could also be achieved by submerging the tip into oil instead of water, which would provide oil-filled tips in the first place. It turned out, however, that Loctite 352 has a relatively strong adhesion to glass compared with oil, which often leaves some glue behind in the tip that finally occludes it. This phenomenon occurred in about 50% of the cases. Water, on the other hand, generates clean pico gauge tips. Other glues, however, might allow the direct production of oil-filled tips.

### Determination of the Bulk Elastic Modulus

To determine the bulk elastic modulus of 10 cSt silicone oil in pico gauges at atmospheric pressure, or 50 cSt silicone oil in pico gauges at 70 kPa (stored in a desiccator at 70 kPa), various pressures between 0.1 and 2.5 MPa were applied in a custom-built microscope pressure chamber that allows microscopic observation of volumetric changes at high resolution. A detailed description of the pressure chamber and measurements is given in Supplemental Appendix S1.

### Pico Gauge Measurement Procedure

The abaxial epidermal layer of a *Vicia faba* leaflet was peeled off and placed cuticle up on an agar plate containing 1% (w/v) agar, 50 mM  $\text{KNO}_3$ , and 1 mM MES buffer, pH 6.15. The plate was transferred to the microscope and exposed to light for 30 min to induce stomatal opening. Observation was carried out with a 63 $\times$  HCX Plan Apo U-V-I water-immersion lens (Leica). A pico gauge produced by method A with a total oil volume of 151 pL was transferred under cold air stream (Supplemental Appendix S1), which was turned off after submersion of the pico gauge tip in the immersion water. The experiment was conducted 1 min after submersion to allow temperature adjustment. Movement of the pico gauge was controlled by a Sutter Instruments model MPC 200 micromanipulator. The pico gauge was impaled into the guard cell while a movie at eight frames per second was taken with a Leica DFC-300 camera attached to a Leica DM LFSa microscope. Consecutive images just before and after impalement were extracted from the movie using ImageJ software (freeware from the National Institutes of Health). Images were opened in

Photoshop software (Adobe). An image taken after the impalement was copied (Ctrl C) and pasted (Ctrl V) into the image taken before impalement (with shortcuts given in parentheses). The opacity of the pasted image was set to 50% to make both images visible, and the overlay was matched using the move tool (V). The area of compression was extracted (Fig. 2D) using the lasso tool (L), filled black using the paint bucket tool (G), and copied (Ctrl C), a new file was opened (Ctrl N), the image was pasted (Ctrl V), layers were merged (Ctrl E), and the image was saved (Ctrl S) as a grayscale .tif file.

To extract volumetric change from the two-dimensional area, a custom-generated software called bubvol (Supplemental Software S1), which generates a solid of revolution and provides the volume, was used. The program can be run under standard software such as MatLab or Octave (freeware; <http://www.gnu.org/software/octave/>). After opening bubvol, the command `V = bubvol('file.tif','')` computes the volume of the image file.tif. Since the images usually have two axes of symmetry, the axis to be computed needs to be indicated roughly by the terms /, -, |, or \. The program finds the exact angle of symmetry and provides a volume in cubic pixels. Adding unit information at the end of the command line (e.g. 4.35) provides the true volume where 1 unit is 4.35 pixels [e.g. `V = bubvol('file.tif','' 4.35)`].

For extraction of total oil volume, an overview image of the total oil volume in the pico gauge was taken and the volume was measured by extracting the area and calculating the volume with bubvol as described above.

The pressure  $\Delta P$  was calculated using Equation 1. The entire process of volume extraction and calculation for one measurement takes about 5 to 10 min.

### Simultaneous Cell Pressure Probe-Pico Gauge Measurement in Onion Epidermis Cells

A custom-built cell pressure probe system constructed after the standard scheme, as described in detail earlier (Hüsken et al., 1978; Tomos, 2000), employing an HPLC valve, peek tubing, 100- $\mu\text{L}$  air-tight Hamilton pipette as pressure piston, and a pressure transducer (Druck Messtechnik), was used for the experiment. The inner epidermis of an onion (*Allium cepa*) bulb was peeled off and placed on an agar plate containing 2% (w/v) agar in distilled water. The plate was placed on the microscope stage, and a drop of distilled water was put between the epidermis and the 63 $\times$  water-immersion lens. A pico gauge with a volume of 1.35 nL was transferred under a cold air stream until it was submerged in the water between the lens and the epidermis, and the air flow was turned off. An oil-filled capillary with about 1- $\mu\text{m}$  tip diameter pulled from borosilicate glass on a Sutter Instruments model P-2000 laser puller was loaded in the cell pressure probe, and the tip was submerged in the immersion water. Both needles were controlled with separate Sutter Instruments model MP-200 micromanipulators. The cell pressure probe tip was pushed against the cell wall of the epidermis cell, and 0.5 MPa prepressure was applied, which equaled the estimated turgor in the cell in order to reduce the influx of cell sap. The needle was impaled, the meniscus was monitored, and counter pressure or tension was applied until the meniscus was in a steady-state position and the pressure indicated on the pressure transducer was recorded. Afterward, the pico gauge was impaled while a movie at eight frames per second was taken. Pico gauge pressure calculations were performed as described above.

### Pico Gauge Measurement in *V. faba* Sieve Elements

Six-week-old *V. faba* plants grown in a greenhouse at 23°C, with 60% to 70% relative humidity and a 14-/10-h light/dark period (daylight plus additional lamp light; model no. PL 90; PL Lighting Systems) with a minimum irradiance of 150  $\text{mmol m}^{-2} \text{s}^{-1}$ , were used for the experiments. Cortical tissue was removed with a razor blade from the midvein of a leaflet as described earlier (Knoblauch and van Bel, 1998). The leaflet was fastened on a microscope stage with double-sided adhesive tape, and the cut was covered with bathing medium consisting of 50 mM KCl, 5 mM NaCl, and 200  $\mu\text{M}$  EDTA. A water-immersion lens (63 $\times$  HCX Plan Apo U-V-I) was dipped into the bathing medium for observation and recording. A pico gauge with a 2.1-nL volume was impaled into the sieve element, and compression of the oil was monitored at eight frames per second with a digital camera. Images were extracted, and volumetric changes were calculated as described above.

### Pico Gauge Measurement in *Alternaria* spp. Hyphae Cells

*Alternaria* spp. hyphae were grown on Glc minimal medium with 1.5% (w/v) agar at 37°C. Just before the experiment, the fungi were covered with liquid Glc minimal medium. Pico gauges manufactured by method B were submerged into



the medium, an appropriate cell was identified using the microscope, and the pico gauge was impaled. Calculation of pressure was performed as described in detail above.

### Supplemental Data

The following materials are available in the online version of this article.

**Supplemental Appendix S1.** Supplemental information on pico gauge production and handling.

**Supplemental Software S1.** Bubvol software.

**Supplemental Image S1.** Test Image 1 for bubvol software.

**Supplemental Image S2.** Test image 2 for bubvol software.

**Supplemental Movie S1.** Pico gauge production method A.

**Supplemental Movie S2.** Pico gauge production method B.

**Supplemental Movie S3.** Pico gauge-cell pressure probe comparison.

**Supplemental Movie S4.** Sieve element turgor measurement.

**Supplemental Movie S5.** Guard cell turgor measurement.

**Supplemental Movie S6.** Fungal hypha turgor measurement.

### ACKNOWLEDGMENTS

We thank the Franceschi Microscopy and Imaging Center (Washington State University) for technical support and Cat Adams (Harvard University) for supplying *Alternaria* spp. cultures.

Received June 24, 2014; accepted September 12, 2014; published September 17, 2014.

### LITERATURE CITED

- Charras GT, Yarrow JC, Horton MA, Mahadevan L, Mitchison TJ (2005) Non-equilibration of hydrostatic pressure in blebbing cells. *Nature* **435**: 365–369
- Cosgrove DJ (1981) Analysis of the dynamic and steady-state responses of growth rate and turgor pressure to changes in cell parameters. *Plant Physiol* **68**: 1439–1446
- Cosgrove DJ (1985) Cell wall yield properties of growing tissue: evaluation by in vivo stress relaxation. *Plant Physiol* **78**: 347–356
- Cosgrove DJ (1993) Wall extensibility: its nature, measurement and relationship to plant cell growth. *New Phytol* **124**: 1–23
- Cosgrove DJ, Ortega JKE, Shropshire W Jr (1987) Pressure probe study of the water relations of *Phycomyces blakesleeanus* sporangiophores. *Biophys J* **51**: 413–423
- Forouzesh E, Goel A, Mackenzie SA, Turner JA (2013) *In vivo* extraction of Arabidopsis cell turgor pressure using nanoindentation in conjunction with finite element modeling. *Plant J* **73**: 509–520
- Franks PJ (2003) Use of the pressure probe in studies of stomatal function. *J Exp Bot* **54**: 1495–1504
- Franks PJ, Buckley TN, Shope JC, Mott KA (2001) Guard cell volume and pressure measured concurrently by confocal microscopy and the cell pressure probe. *Plant Physiol* **125**: 1577–1584
- Franks PJ, Cowan IR, Farquhar GD (1998) A study of stomatal mechanics using the cell pressure probe. *Plant Cell Environ* **2**: 94–100
- Gómez-Martínez R, Hernández-Pinto AM, Duch M, Vázquez P, Zinoviev K, de la Rosa EJ, Esteve J, Suárez T, Plaza JA (2013) Silicon chips detect intracellular pressure changes in living cells. *Nat Nanotechnol* **8**: 517–521
- Harold RL, Money NP, Harold FM (1996) Growth and morphogenesis in *Saprolegniaferax*: is turgor required? *Protoplasma* **191**: 105–114
- Howard RJ, Ferrari MA, Roach DH, Money NP (1991) Penetration of hard substrates by a fungus employing enormous turgor pressures. *Proc Natl Acad Sci USA* **88**: 11281–11284
- Hüsken D, Steudle E, Zimmermann U (1978) Pressure probe technique for measuring water relations of cells in higher plants. *Plant Physiol* **61**: 158–163
- Knoblauch M, Noll GA, Müller T, Prüfer D, Schneider-Hüther I, Scharner D, Van Bel AJE, Peters WS (2003) ATP-independent contractile proteins from plants. *Nat Mater* **2**: 600–603
- Knoblauch M, Peters WS (2010) Münch, morphology, microfluidics: our structural problem with the phloem. *Plant Cell Environ* **33**: 1439–1452
- Knoblauch M, Peters WS, Ehlers K, van Bel AJE (2001) Reversible calcium-regulated stopcocks in legume sieve tubes. *Plant Cell* **13**: 1221–1230
- Knoblauch M, van Bel AJE (1998) Sieve tubes in action. *Plant Cell* **10**: 35–50
- Mine I, Menzel D, Okuda K (2008) Morphogenesis in giant-celled algae. *Int Rev Cell Mol Biol* **266**: 37–83
- Money NP, Harold FM (1992) Extension growth of the water mold *Achlya*: interplay of turgor and wall strength. *Proc Natl Acad Sci USA* **89**: 4245–4249
- Münch E (1930). *Die Stoffbewegung in der Pflanze*. Fischer, Jena, Germany
- Oparka KJ, Murphy R, Derrick PM, Prior DAM, Smith JAC (1991) Modification of the pressure-probe technique permits controlled intracellular microinjection of fluorescent probes. *J Cell Sci* **98**: 539–544
- Shackel KA, Brinckmann E (1985) In situ measurement of epidermal cell turgor, leaf water potential, and gas exchange in *Tradescantia virginiana* L. *Plant Physiol* **78**: 66–70
- Steudle E, Zimmermann U (1977) Effect of turgor pressure and cell size on the wall elasticity of plant cells. *Plant Physiol* **59**: 285–289
- Stewart MP, Helenius J, Toyoda Y, Ramanathan SP, Muller DJ, Hyman AA (2011) Hydrostatic pressure and the actomyosin cortex drive mitotic cell rounding. *Nature* **469**: 226–230
- Timoshenko S (1951) *Theory of Elasticity*. McGraw-Hill, New York
- Tomos AD (2000) The plant cell pressure probe. *Biotechnol Lett* **22**: 437–442
- Tomos AD, Leigh RA (1999) The pressure probe: a versatile tool in plant cell physiology. *Annu Rev Plant Physiol Plant Mol Biol* **50**: 447–472
- Wada H, Fei J, Knipfer T, Matthews MA, Gambetta G, Shackel K (2014) Polarity of water transport across epidermal cell membranes in *Tradescantia virginiana*. *Plant Physiol* **164**: 1800–1809
- Ye Q, Steudle E (2006) Oxidative gating of water channels (aquaporins) in corn roots. *Plant Cell Environ* **29**: 459–470